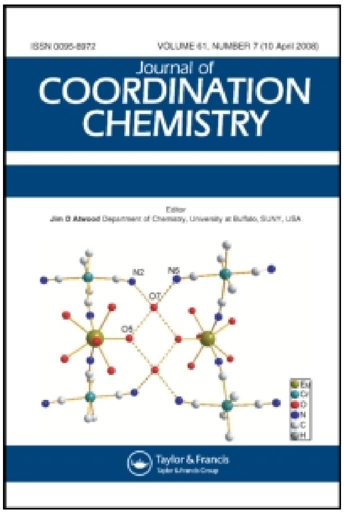

Journal of Coordination Chemistry
Publication details, including instructions for authors and subscription information:
http://www.informaworld.com/smpp/title~content=t713455674

A novel inorganic-organic hybrid based on a Wells-Dawson polyanion containing two types of organic fragments

Ai-Xiang Tian[a]; Zhan-gang Han[b]; Jun Peng[a]; Jiang-li Zhai[a]; Bao-xia Dong[a]; Jing-quan Sha[a]
[a] Key Laboratory of Polyoxometalate Science, Ministry of Education, Faculty of Chemistry, Northeast Normal University, Changchun, P.R. China [b] Faculty of Chemistry, Hebei Normal University, Shijiazhvang, Hebei, P.R. China

To cite this Article Tian, Ai-Xiang , Han, Zhan-gang , Peng, Jun , Zhai, Jiang-li , Dong, Bao-xia and Sha, Jing-quan(2007) 'A novel inorganic-organic hybrid based on a Wells-Dawson polyanion containing two types of organic fragments', Journal of Coordination Chemistry, 60: 15, 1645 — 1654

To link to this Article: DOI: 10.1080/00958970601099829

URL: http://dx.doi.org/10.1080/00958970601099829

Journal of Coordination Chemistry
Vol. 60, No. 15, 1 August 2007, 1645–1654

Taylor & Francis
Taylor & Francis Group

A novel inorganic-organic hybrid based on a Wells–Dawson polyanion containing two types of organic fragments

AI-XIANG TIAN†, ZHAN-GANG HAN‡, JUN PENG*†, JIANG-LI ZHAI†,
BAO-XIA DONG† and JING-QUAN SHA†

†Key Laboratory of Polyoxometalate Science, Ministry of Education, Faculty of Chemistry,
Northeast Normal University, Changchun, 130024, P.R. China
‡Faculty of Chemistry, Hebei Normal University, Shijiazhvang, Hebei, P.R. China

(*Received 24 July 2006; revised 6 September 2006; in final form 7 September 2006*)

A new inorganic-organic hybrid, $[Zn(phen)_2(ppy)][\{Zn(phen)_2\}\{Zn(phen)_2(H_2O)\}\{P_2W_{18}O_{62}\}]\cdot 2H_2O$ (phen = 1,10′-phenanthroline, ppy = 2-(5-phenylpyridin-2-yl)pyridine) (**1**), by using pre-prepared Wells–Dawson salt α-$K_6P_2W_{18}O_{62}\cdot 15H_2O$ as precursor, has been synthesized under hydrothermal conditions. Compound **1** was characterized by single-crystal X-ray diffraction, elemental analyses, IR spectrum and cyclic voltammetry. Yellow crystals crystallized in the monoclinic space group $P2\ (1)/c$ with $a = 16.2450(11)$ Å, $b = 17.0918(11)$ Å, $c = 43.640(3)$ Å, $\beta = 92.0060(10)^\circ$, $V = 12109.4(14)$ Å^3, $Z = 4$. The title compound represents a novel zero-dimensional structure based on bisupporting Wells–Dawson POM: one terminal oxygen atom located in the "belt" site and another located in the "cap" site of the same hemisphere of the polyanion are coordinated by Zn^{2+} cations. Compound **1** also contains the isolated secondary metal complex $[Zn(phen)_2(ppy)]^{2+}$ with two different organic ligands phen and ppy.

Keywords: Wells–Dawson; Pre-prepared polyoxometalate; Hydrothermal synthesis; Transition metal complex

1. Introduction

Polyoxometalates (POMs) attract considerable attention because of the structural versatility and also their potential applications in catalysis, electrical conductivity and biological chemistry [1]. POM chemistry has been enriched since secondary metal coordination complexes have been introduced into POMs as charge compensation or grafted on the inorganic POM framework itself [2]. Many of these hybrids are based on classical POMs, such as Keggin [3], Anderson [4] and Lindqvist [5]. Wells–Dawson polyoxoanion-supported metal complexes have not been extensively studied. Incorporation of lanthanides or their coordination complexes into Wells–Dawson polyanions, involve discrete structures [6], 1 : 1, 1 : 2 and 2 : 2 type dimers [7], and the dimensionally expanded structures [6a, 8]. In contrast, hybrids based on Wells–Dawson POMs and TM (TM = transition metal) complexes are rare. Only a few examples are reported, $[Cu(en)_2(OH_2)]_2[H_2en][\{Cu(en)_2\}P_2CuW_{17}O_{61}]\cdot 5H_2O$,

---

*Corresponding author. Tel.: +86 431509965. Fax: +86 43-5099667. Email: jpeng@nenu.edu.cn

Journal of Coordination Chemistry
ISSN 0095-8972 print/ISSN 1029-0389 online © 2007 Taylor & Francis
DOI: 10.1080/00958970601099829

$[Cu(en)_2(OH_2)]_2[Cu(en)_2]_{0.5}[H_2en]_{0.5}[\{Cu(en)_2\}P_2CuW_{17}O_{61}] \cdot 5H_2O$ [9], and $[\{Cu_2(2,4'\text{-}Hbpy)_4\}Mo_{18}As_2O_{62}] \cdot 2H_2O$ [10], which have 1D chain structures.

Herein, $[Zn(phen)_2(ppy)][\{Zn(phen)_2\}\{Zn(phen)_2(H_2O)\}\{P_2W_{18}O_{62}\}] \cdot 2H_2O$ (phen = 1,10′-phenanthroline, ppy = 2-(5-phenylpyridin-2-yl)pyridine) (**1**), was synthesized by using $\alpha\text{-}K_6P_2W_{18}O_{62}\cdot 15H_2O$ as precursor under hydrothermal conditions, which contains two $[Zn(phen)_2]^{2+}$ subunits coordinating a terminal oxygen located in the "belt" site and a bridging oxygen located in the "cap" site of the same hemisphere of the polyanion; an isolated secondary metal complex $[Zn(phen)_2(ppy)]^{2+}$ with two different ligands (phen and ppy), acts as a compensating cation.

2. Experimental section

2.1. *Materials and methods*

All reagents were reagent grade and used as received from commercial sources without further purification. The $\alpha\text{-}K_6P_2W_{18}O_{62} \cdot 15H_2O$ was prepared according to the literature method [11] and verified by IR spectrum. Organic ppy was synthesized in the laboratory and confirmed by ^1H NMR and IR. Elemental analyses (C, H and N) were performed on a Perkin–Elmer 2400 CHN elemental analyzer. The IR spectrum was obtained on an Alpha Centaurt FT/IR spectrometer with KBr pellet in the 400–4000 cm^{-1} region. Electrochemical measurements were performed with a CHI 660b electrochemical workstation. A conventional three-electrode system was used. The working electrode was a modified carbon paste electrode (CPE). Ag/AgCl (3 M KCl) electrode was used as a reference electrode and a Pt wire as a counter electrode.

2.2. *Hydrothermal synthesis*

A mixture of $\alpha\text{-}K_6P_2W_{18}O_{62} \cdot 15H_2O$ (0.32 g), $ZnCl_2$ (0.23 g), phen (0.05 g), ppy (0.01 g), and H_2O (10 mL) was stirred for half an hour in air. The mixture was then transferred to a Teflon-lined stainless steel autoclave (20 mL) and kept at 170°C for 4 days. After the autoclave had cooled to room temperature over 12 h, yellow block-shaped crystals of **1** were filtered off, washed with distilled water, and air-dried to give a yield of 30% based on W. Anal. Calcd for $C_{88}N_{14}H_{66}Zn_3P_2W_{18}O_{65}$ **1** (%): C, 17.82; H, 1.11; N, 3.31. Found: C, 17.90; H, 1.18; N, 3.25.

2.3. *X-ray crystallography*

A suitable single crystal of **1** (with dimensions $0.24 \times 0.20 \times 0.12\,mm^3$) was glued on a glass fiber. Data were collected on a CCD diffractometer with graphite-monochromated Mo-K_α radiation ($\lambda = 0.71703$ Å) at 293 K. A total of 61,179 reflections were collected in the range $1.51° < \theta < 25°$ ($-9 \le h \le 16$, $-19 \le k \le 20$, $-5 \le l \le 47$), of which 21,318 are unique ($R_{int} = 0.0603$) and 16,119 with $I > 2\sigma(I)$ were used in the refinement of the structure of **1**. The structure was refined by full-matrix least-squares on F^2 using the SHELXTL crystallographic software package [12]. Anisotropic thermal parameters were used to refine all non-hydrogen atoms except several oxygen, carbon and nitrogen atoms. Hydrogen atoms were located at their ideal positions as a riding mode. The crystal data and structure refinement of compound **1** were summarized in table 1. Selected bond lengths (Å) and angles (°) were listed in table 2.

The CCDC reference numbers is 61 1537 for **1**. These data can be obtained free of charge from the Cambridge Crystallographic Data Centre *via* www.ccdc.cam.ac.uk/data_request/cif

Table 1. Crystal data and structure refinement for **1**.

Formula	$C_{88}N_{14}H_{66}Zn_{3\text{-}}P_{2}W_{18}O_{65}$
FW	5926.93
T (K)	293(2)
Crystal system	Monoclinic
Space group	$P2(1)/c$
a (Å)	16.2450(11)
b (Å)	17.0918(11)
c (Å)	43.640(3)
α (°)	90.00
β (°)	92.0060(10)
γ (°)	90.00
V (Å^3)	12109.4(14)
Z	4
D_c (g cm^{-3})	3.248
μ (mm^{-1})	17.726
Final R_1^{a}, wR_2^{b} [$I > 2\sigma(I)$]	0.0711, 0.1877
Final R_1^{a}, wR_2^{b} (all data)	0.0960, 0.1974
GOF on F^2	1.062

$^a R_1 = \Sigma\|Fo| - |Fc\|/\Sigma|Fo|$.
$^b wR_2 = \Sigma\|[w(Fo^2 - Fc^2)^2]/\Sigma(w(Fo^2)^2]^{1/2}$.

Table 2. Selected bond lengths (Å) and bond angles (°) for **1**.

W(1)–O(17)	1.713(19)	W(2)–O(23)	1.696(17)
W(1)–O(11)	1.886(15)	W(2)–O(22)	1.845(14)
W(1)–O(46)	1.922(15)	W(2)–O(48)	1.862(15)
W(1)–O(35)	1.922(14)	W(2)–O(27)	1.937(17)
W(1)–O(62)	1.924(17)	W(2)–O(12)	1.974(16)
W(1)–O(6)	2.384(16)	W(2)–O(2)	2.361(16)
O(31)–Zn(1)	2.233(16)	O(12)–Zn(3)	2.060(16)
N(3)–Zn(1)	2.13(2)	N(1)–Zn(3)	2.00(2)
N(4)–Zn(1)	2.16(2)	N(2)–Zn(3)	2.15(2)
N(9)–Zn(1)	2.10(2)	N(6)–Zn(3)	2.15(2)
N(10)–Zn(1)	2.15(3)	N(8)–Zn(2)	2.13(2)
N(7)–Zn(2)	2.17(2)	N(14)–Zn(2)	2.18(3)
N(13)–Zn(2)	2.12(3)	N(12)–Zn(2)	2.29(2)
N(11)–Zn(2)	2.11(2)		
N(5)–Zn(3)	2.05(2)	N(9)–Zn(1)–N(3)	170.5(9)
N(3)–Zn(1)–N(10)	96.5(11)	N(9)–Zn(1)–N(10)	77.4(10)
N(3)–Zn(1)–OW1	93.9(9)	N(9)–Zn(1)–OW1	91.6(9)
N(3)–Zn(1)–N(4)	80.2(8)	N(10)–Zn(1)–OW1	168.2(10)
N(9)–Zn(1)–O(31)	91.9(8)	N(10)–Zn(1)–N(4)	89.9(8)
N(9)–Zn(1)–N(4)	92.4(8)	OW1–Zn(1)–N(4)	86.4(7)
N(3)–Zn(1)–O(31)	95.8(8)	N(10)–Zn(1)–O(31)	94.5(8)
N(4)–Zn(1)–O(31)	174.4(7)	OW1–Zn(1)–O(31)	90.0(7)

2.4. *Preparation of carbon paste electrode modified by compound 1 (1-CPE)*

Compound **1** modified CPE (**1**-CPE) was fabricated by the following process: 0.05 g **1** and 0.5 g graphite powder were mixed and ground together by an agate mortar and pestle to achieve an even, dry mixture; to the mixture 0.5 mL paraffin oil was added and stirred with a glass rod; then the mixture was prepared to pack into 3 mm inner diameter glass tube, and the surface was pressed tightly onto weighing paper with a copper rod through the back. Electrical contact was established with a copper rod through the back of the electrode.

3. Results and discussion

3.1. *Structure description*

Compound **1** is constructed from Wells–Dawson polyoxoanion α-$[P_2W_{18}O_{62}]^{6-}$ and Zn-organic complex building blocks. The heteropolyanion of the title compound retains the parent structure which contains two $[\alpha\text{-A-}PW_9O_{34}]^{9-}$ units derived from α-Keggin type anion by removal of a set of three corner-shared WO_6 octahedra. The polyanion itself is close to D_{3h} point symmetry, containing two categories of W atoms: six at 'polar' positions and twelve at 'equator' positions [13]. For **1**, W–O distances are 1.678(17)−1.748(17) Å for terminal oxygen atoms, 1.845(14)−1.988(15) Å for μ_2-bridging oxygen atoms, 2.321(15)−2.441(19) Å for μ_3-bridging oxygen atoms, respectively.

Single-crystal X-ray structural analysis reveals that **1** contains one bisupporting $[\{Zn(phen)_2\}\{Zn(phen)_2(H_2O)\}\{P_2W_{18}O_{62}\}]^{2-}$ polyoxoanion, one discrete [Zn(phen)$_2$] (ppy)]$^{2+}$ cation and two water molecules (see figure 1). Three crystallographically independent Zn centers have different coordination environments. Both Zn(1) and Zn(2) are six-coordinate while Zn(3) is five-coordinate. Zn(1) is coordinated by four nitrogen atoms (N3, N4, N9 and N10) from two phen ligands with Zn–N distances of 2.10(2)–2.16(2) Å, one water molecule (OW1) with Zn–OW distance of 2.156(19) Å and one terminal oxygen atom (O31) of α-$[P_2W_{18}O_{62}]^{6-}$ cluster with Zn–O distance of 2.233(16) Å. Zn(2) is coordinated by two kinds of organic ligands: four nitrogen atoms (N7, N8, N13 and N14) from two phens with Zn–N distances of 2.12(3)–2.18(3) Å; two nitrogen atoms (N11 and N12) from one ppy with Zn–N distances of 2.11(2) and 2.29(2) Å. Zn(3) is coordinated by four nitrogen atoms (N1, N2, N5 and N6) from two phens with Zn–N distances of 2.00(2)–2.15(2) Å, one bridging oxygen atom (O12) from polyoxoanion cluster with Zn–O distance 2.060(16) Å. Supramolecular interactions endow compound **1** with a striking feature. The coordinated water molecules OW1 and crystal water molecules OW2 link adjacent polyanions $[\{Zn(phen)_2\}\{Zn(phen)_2(H2O)\}\{P_2W_{18}O_{62}\}]^{2-}$ together through hydrogen bonding interactions with OW1 $\cdots$ O9 = 2.793 Å, OW1 $\cdots$ O47 = 2.992 Å, OW2 $\cdots$ O18 = 2.878 Å, and OW2 $\cdots$ O20 = 3.027 Å. Thus, 1D supramolecular left- and right-handed helical chains in pairs are formed via hydrogen bonding interactions, similar to the covalent bonding $[\{L/D\text{–}Cd(H_2O)(phen)_2\}_2\{V_{16}O_{38}(Cl)\}]$ chains and supramolecular helical chains of $(Hbpy)_4[SiMo_{12}O_{40}]$ [14]. The adjacent supramolecular helical chains are further connected together by OW3′ molecules through hydrogen bonding interactions with OW3′ $\cdots$ O25 = 2.539,

$OW3' \cdots O30 = 3.026$ Å to construct 2D supramolecular networks, leaving micropores to accommodate discrete subunits $[Zn(phen)_2(ppy)]^{2+}$ (see figure 2).The $\pi \cdots \pi$ contacts between ppy's and phen's form offset face-to-face and edge-to-face stacking styles (see figure S1). Aryl packing and hydrogen bonding interactions lead to the formation of a 3D supramolecular framework of compound **1**.

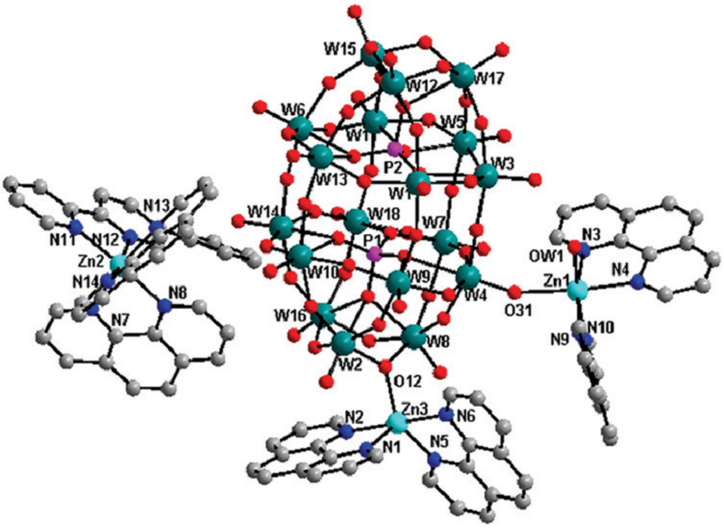

Figure 1. Molecular drawing of **1** with atom labels. All hydrogen atoms and water molecules are omitted for clarity.

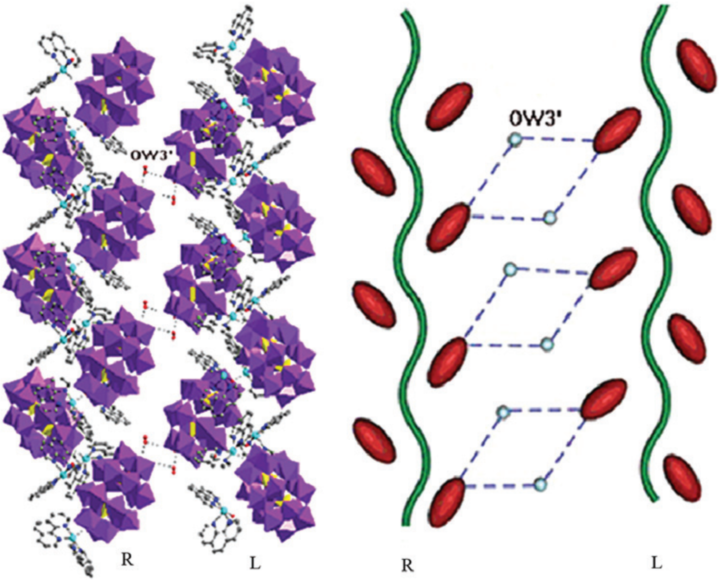

Figure 2. Polyhedral view (left) and schematic illustration (right) of the 2D supramolecular network formed by the 1D supramolecular chains (R: right-handed chain, L: left-handed chain). All hydrogen atoms and discrete units $[Zn(phen)_2(ppy)]^{2+}$ are omitted for clarity.

In compound **1**, the structural features lie in two points: firstly, the mixed organic ligands ppy and phen coexist; secondly, Zn(1) and Zn(3) coordination ions covalently bond to one "belt" terminal oxygen atom and one "cap" bridging oxygen atom of the same hemisphere to form two "arms" on the anion.

3.2. *FT-IR spectrum*

The IR spectrum of **1** exhibits a band at $1095\,\mathrm{cm}^{-1}$ attributed to ν(P–O) and characteristic bands at 960, 910, and $786\,\mathrm{cm}^{-1}$ attributed to ν(W=O) and ν(W–O–W); the compound also shows characteristic bands at 1427, 1517, and $1623\,\mathrm{cm}^{-1}$ associated with the phen and ppy ligands (see figure S2).

3.3. *Voltammetric behavior of* **1**-*CPE in aqueous electrolyte*

The cyclic voltammogram for **1**-CPE in 1 M H_2SO_4 aqueous solution at a scan rate of $60\,\mathrm{mV \cdot s^{-1}}$ is presented in figure 3. Three reversible redox peaks appear from 0 to –700 mV. The half-wave potentials $E_{1/2} = (E_{pa} + E_{pc})/2$ are −165(I), −382(II) and −615(III) mV for **1**-CPE. The pairs of redox peaks I–I′, II–II′ and III–III′ should be attributed to three consecutive two-electron processes of W(VI). The values of peak-to-peak separation between the corresponding anodic and cathodic peaks (ΔE_p) are 34 mV for I–I′, 25 mV for II–II′ and 43 mV for III–III′.

The cyclic voltammograms for **1**-CPE in 1M H_2SO_4 aqueous solution at different scan rates in the potential range of 0−700 mV are presented in figure 4. When the scan rate is varied from 60 to $500\,\mathrm{mV \cdot s^{-1}}$, the peak potentials change gradually following the scan rates: the cathodic peak potentials shift negative and the corresponding anodic peak potentials positive [15]. When the scan rates are lower than $180\,\mathrm{mV \cdot s^{-1}}$, the peak currents are proportional to the scan rates, which indicates that the redox process

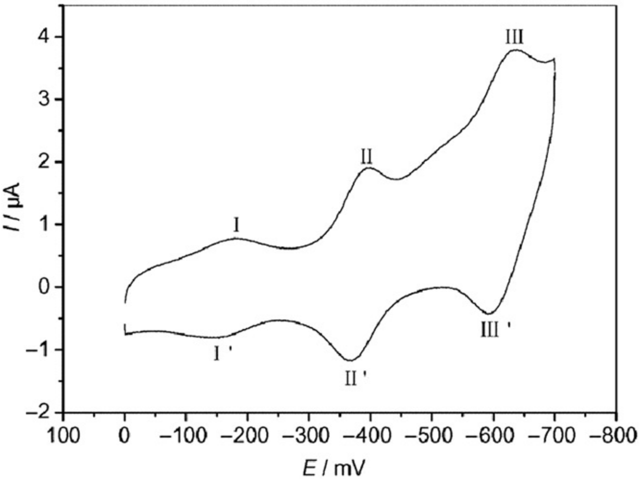

Figure 3. Cyclic voltammogram of **1**-CPE in 1M H_2SO_4 at a scan rate of $60\,\mathrm{mV \cdot s^{-1}}$.

of **1**-CPE is surface-controlled; however, when the scan rates are higher than $180\,\mathrm{mV \cdot s^{-1}}$, the peak currents are proportional to the square root of the scan rates, which indicates that the redox process of **1**-CPE is diffusion-controlled (see figure S3).

3.4. *pH-dependent electrochemical behavior of the 1-CPE*

The pH of the supporting electrolyte has a remarkable effect on the electrochemical behavior of the **1**-CPE in $H_2SO_4 + Na_2SO_4$ aqueous solutions. As can be seen from figure 5a, following the increase of the pH, all three waves shift to more negative

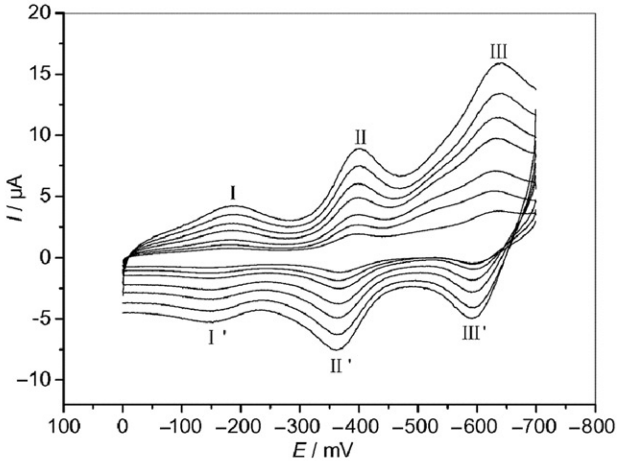

Figure 4. The cyclic voltammograms of **1**-CPE in 1M H_2SO_4 at different scan rates (from inner to outer: 60, 100, 140, 220, 300, 400, $500\,\mathrm{mV \cdot s^{-1}}$).

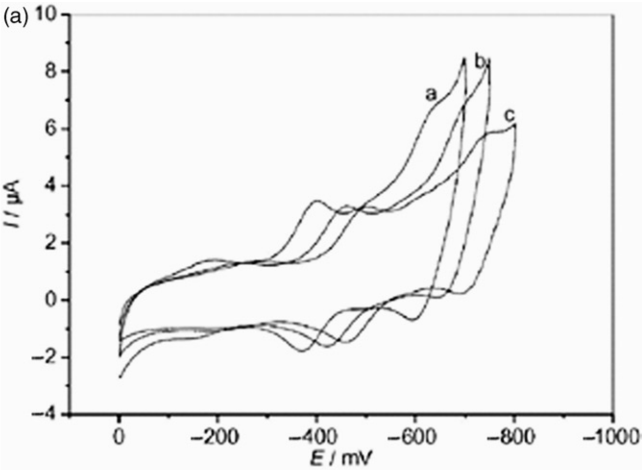

Figure 5. (a) The cyclic voltammograms for **1**-CPE in $H_2SO_4 + Na_2SO_4$ solutions with different pH: (a) 0.63; (b) 1.59; (c) 2.02. (b) The relationship of peak potential and pH. Scan rate: $100\,\mathrm{mV \cdot s^{-1}}$.

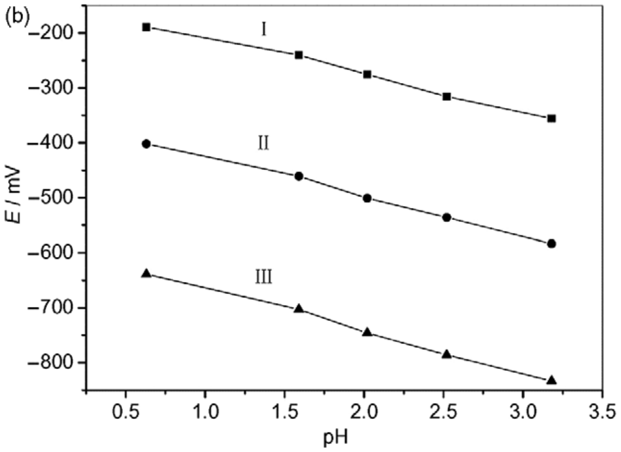

Figure 5. Continued.

potentials and the peak currents decrease. The potentials and current changes mentioned above can be explained by the Nernst equation and Fick's first law [16]. Plots of peak potentials of three redox waves *versus* pH for the **1**-CPE show good linearity in the pH range from 0.63 to 2.02 (see figure 5b). Slopes of the pH range are −66, −72, and −75 mV/pH for the three peak couples, respectively, coorresponding to the addition of aproximately two protons [17].

3.5. *Stability and surface-renewal of 1-CPE*

In our experiment, we found that **1**-CPE showed higher stability. When the potential range is maintained at 0 to –700 mV, it is stable over 500 cycles at a rate of $100\,\mathrm{mV\cdot s^{-1}}$ and the current response remained almost unchanged. When **1**-CPE was stored at room temperature (20−30°C) for at least one month, there is negligible change in the shape and height of the redox waves. The remarkable stability of **1**-CPE should be ascribed to the insolubility of the inorganic-organic hybrid POM synthesized under hydrothermal conditions. The advantage of using the bulk-modified electrode is that the electrode surface can be renewed by squeezing a little carbon paste out of the tube when needed, which is especially useful for electrocatalytic study since the catalytic activity is known to decrease when the electrode is dirty.

4. Conclusion

In this article, **1** was synthesized under hydrothermal conditions by using pre-prepared Dawson-type salt α-$K_6P_2W_{18}O_{62}\cdot 15H_2O$ as precursor. The Zn(1) and Zn(3) coordination centers covalently bond to one "belt" terminal oxygen atom and one "cap" bridging oxygen atom of the same hemisphere to form pendants grafted on the anion. The discrete metal-organic complex contains two types of organic ligands. Combining the aryl packing and hydrogen bonding interactions, a 3D supramolecular framework is formed.

Acknowledgment

This work was financially supported by the Natural Science Foundation of China (20271001).

References

[1] (a) M.T. Pope. *Heteropoly- and Isopoly Oxometalates*, Springer-Verlag, Berlin (1983); (b) C.L. Hill. *Chem. Rev*. **98**, 1 (1998); (c) M.T. Pope, A. Müller (Eds), *Polyoxometalate Chemistry: From Topology Via Self-Assembly to Applications, Kluwer Academic*, Dordrecht, The Netherlands (2001); (d) M.T. Pope, A. Müller. *Angew. Chem. Int. Ed.* **30**, 34 (1991); (e) W.B.Yang, C.Z. Lu. *Inorg. Chem*., **41**, 5638 (2002).

[2] (a) L.S. Felices, P. Vitoria, J.M. Gutiérrez-Zorrilla, S. Reinoso, J. Etxebarria, L. Lezama. *Chem. Eur. J*., **10**, 5138 (2004); (b) D. Hagrman, P.J. Hagrman, J. Zubieta. *Angew. Chem. Int. Ed*., **38**, 3165 (1999); (c) S.X. Liu, L.H. Xie, B. Gao, C.D. Zhang, C.Y. Sun, D.H. Li, Z.M. Su. *Chem. Commun*., **40**, 5023 (2005); (d) S. Reinoso, P. Vitoria, J.M. Gutiérrez-Zorrilla, L. Lezama, L.S. Felices, J.I. Beitia. *Inorg. Chem*., **44**, 9731 (2005).

[3] (a) H.Y. An, E.B. Wang, D.R. Xiao, Y.G. Li, Z.M. Su, L. Xu. *Angew. Chem. Int. Ed*., **45**, 904 (2006); (b) C.M. Liu, D.Q. Zhang, D.B. Zhu. *Cryst. Growth Des*., **6**, 524 (2006); (c) W.S. You, E.B. Wang, Y. Xu, Y.G. Li, L. Xu, C.W. Hu. *Inorg. Chem*., **40**, 5468 (2001); (d) Y.P. Ren, X.J. Kong, L.S. Long, R.B. Huang, L.S. Zheng. *Cryst. Growth Des*., **6**, 572 (2006).

[4] (a) H.Y. An, Y.G. Li, E.B. Wang, D.R. Xiao, C.Y. Sun, L. Xu. *Inorg. Chem*., **44**, 6062 (2005); (b) V. Shivaiah, S.K. Das. *Inorg. Chem*., **44**, 8846 (2005); (c) V. Shivaiah, P.V.N. Reddy, L. Cronin, S.K. J. Das. *Chem. Soc. Dalton Trans*., **20** 3781 (2002); (d) D. Drewes, E.M. Limanski, B.J. Krebs. *Chem. Soc. Dalton Trans*., **14**, 2087 (2004).

[5] (a) J.H. Kang, J.A. Nelson, M. Lu, B.H. Xie, Z.H. Peng, D.R. Powell. *Inorg. Chem*., **43**, 6408 (2004); (b) Y.G. Li, E.B. Wang, S.T. Wang, Y. Lu, C.W. Hu, N.H. Hu, H.Q. Jia. *J. Mol. Struct*., **607**, 133 (2002); (c) J.H. Kang, B.B. Xu, Z.H. Peng, X.D. Zhu, Y.G. Wei, D.R. Powell. *Angew. Chem. Int. Ed*., **117**, 7062 (2005).

[6] (a) J.Y. Niu, D.G. Guo, J.W. Zhao, J.P. Wang. *New. J. Chem*., **28**, 980 (2004); (b) Wang, J.P.; Guo, D.G.; Niu, J.Y. Chin. *J. Inorg. Chem*., **19**, 579 (2003).

[7] (a) M. Sadakane, M.H. Dickman, M.T. Pope. *Inorg. Chem*., **40**, 2715 (2001); (b) Q.H. Luo, R.C. Howell, J. Bartis, M. Dankova, W.D. Horrocks, A.L. Rheingold, L.C. Francesconi. *Inorg. Chem*., **41**, 6112 (2002); (c) Q.H. Luo, R.C. Howell, M. Dankova, J. Bartis, C.W. Williams, W.D. Horrocks, V.G. Young, A.L. Rheingold, L.C. Francesconi, M.R. Antonio. *Inorg. Chem*., **40**, 1894 (2001); (d) J.Y. Niu, J.W. Zhao, D.J. Guo, J.P. Wang. *J. Mol. Struct*., **692**, 223 (2004); (e) C. Boglio, G. Lenoble, C. Duhayon, B. Hansenknopf, R. Thouvenot, C. Zhang, R.C. Howell, B.P. Burton-Pye, L.C. Francesconi, E. Lacôte, L. horimbert, T.M. Malacria, C. Afonso, J.C. Tabet. *Inorg. Chem*., **45**, 1389 (2006).

[8] (a) Y. Lu, Y. Xu, Y.G. Li, E.B. Wang, X.X. Xu, Y. Ma. *Inorg. Chem*., **45**, 2055 (2006); (b) J.Y. Niu, D.J. Guo, J.P. Wang, J.W. Zhao. *Cryst. Growth Des*., **4**, 241 (2004); (c) J.P. Wang, J.W. Zhao, J.Y. Niu. *J. Mol. Struct*., **697**, 191 (2004).

[9] B.B. Yan, Y. Xu, X.H. Bu, N.K. Goh, L.S. Chia, G.D. Stucky. *J. Chem. Soc. Dalton Trans*., **13**, 2009 (2001).

[10] T. Soumahoro, E. Burkholder, W. Ouellette, J. Zubieta. *Inorg. Chem. Commun*., **358**, 606 (2005).

[11] D.K. Lyon, W.K. Miller, T. Novet, P.J. Domaille, E. Evitt, D.C. Johnson, R.G. Finke. *J. Am. Chem. Soc*., **113**, 7209 (1991).

[12] (a) G.M. Sheldrick. SHELXS-97, *Program for Crystal Structure Solution*, University of Göttingen, Germany, 1997; (b) G.M. Sheldrick. SHELXL-97, *Program for Crystal Structure Refinement*, University of Göttingen, Germany, 1997.
[13] L.E. Briand, G.T. Baronetti, H.J. Thomas. *Appl. Catal. A: Gen.*, **256**, 37 (2003).
[14] (a) Z.G. Han, Y.L. Zhao, J. Peng, Q. Liu, E.B. Wang. *Electrochim. Acta*, **51**, 218 (2005); (b) Y.H. Chen, J. Peng, H.Q. Yu, Z.G. Han, X.J. Gu, Z.S. Shi, E.B. Wang, N.H. Hu. *Inorg. Chim. Acta*, **358**, 403 (2005).
[15] M. Sadakane, E. Steckhan. *Chem. Rev.*, **98**, 219 (1998).
[16] J. Wang. *Analytical Electrochemistry*, p. 124, VCH, New York (1994).
[17] (a) N. Fay, E. Dempsey, T. McCormac. *J. Electroanal. Chem.*, **574**, 359 (2005); (b) N. Fay, E. Dempsey, A. Kennedy, T. McCormac. *J. Electroanal. Chem.*, **556**, 63 (2003).